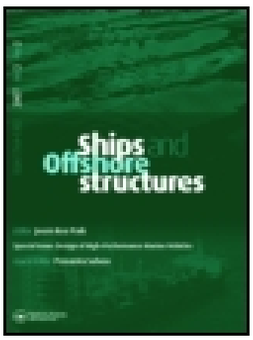

Taylor & Francis
Taylor & Francis Group

Ships and Offshore Structures

ISSN: (Print) (Online) Journal homepage: https://www.tandfonline.com/loi/tsos20

Assessment of the technical safe limit speed of a non-ice-strengthened naval vessel with representative and alternative side shell designs in ice-infested waters

Mark Bobeldijk, Sander Dragt, Martijn Hoogeland & Jan van Bergen

To cite this article: Mark Bobeldijk, Sander Dragt, Martijn Hoogeland & Jan van Bergen (2021): Assessment of the technical safe limit speed of a non-ice-strengthened naval vessel with representative and alternative side shell designs in ice-infested waters, Ships and Offshore Structures, DOI: 10.1080/17445302.2021.1912475

To link to this article: https://doi.org/10.1080/17445302.2021.1912475

SHIPS AND OFFSHORE STRUCTURES
https://doi.org/10.1080/17445302.2021.1912475

Taylor & Francis
Taylor & Francis Group

Assessment of the technical safe limit speed of a non-ice-strengthened naval vessel with representative and alternative side shell designs in ice-infested waters

Mark Bobeldijk [a], Sander Dragt[a], Martijn Hoogeland[a] and Jan van Bergen[b]

[a]Department of Structural Dynamics (SD), TNO, Delft, The Netherlands; [b]Department of Maritime Systems, Defence Materiel Organisation (DMO), Utrecht, The Netherlands

ABSTRACT

Sailing in ice-infested waters has become more relevant for the Royal Netherlands Navy (RNLN). A method is developed to determine the technical safe speed for a single ice floe impact with a typical non-ice strengthened naval vessel. A representative ice floe impact load scenario is applied to three structural arrangements for the side shell structure: a reference design and two alternative Lean Duplex designs. Practical visual and structural acceptance criteria are defined. The proposed changes to the structural layout and the material will improve the ability to resist floe impacts at higher sailing speeds. The first exceedance of a visual criterion is improved from 1 m/s to 2 m/s. The more severe structural criterion is not exceeded at all, while this was the case for the reference design (at 2 m/s). Nevertheless, permanent deformations, are to be expected when these non-ice strengthened ships are operating in ice-infested waters.

ARTICLE HISTORY
Received 5 November 2020
Accepted 23 March 2021

KEYWORDS
ice belt; Lean Duplex (EN1.4062); ice floe impact; non-ice-strengthened naval vessel

1. Introduction

The effects of climate change are visible through the retraction of the ice infested zone in polar waters. This allows for a larger window of operation for nautical operations in the Arctic and near-Arctic regions. As a result, the Royal Netherlands Navy (RNLN) investigates the technical consequences of incidental operations in the marginal ice zone (MIZ) for possible search and rescue operations, with non-ice strengthened naval vessels. This scenario will expose the vessel to ship-ice collision events, for which it is essential to define criteria for the technical safe operation, as a basis for operational guidelines.

A Popov based technical methodology has been used in Dolny (2017, 2018) for assessing ice-ship collision. An analytical method is used to determine the contact area and pressure, where the Finite Element Method (FEM) is used to assess the structural response to the contact. This method has been used by Dolny (2017) for a case study of a 140 m 5000 ton PC5 patrol vessel and by Daley (2015) for a 150 m 8000 ton displacement notional destroyer. This method will also be used for the present work.

Work by Quinton and Daley (2010; Quinton et al. 2012) shows that a moving (sliding) load may cause significantly more structural damage than a static load. Therefore, it is more appropriate to consider a moving instead of a static load, as will be used in this paper.

In this paper, the structural response of a typical non-ice strengthened 140 m long naval vessel to an impact with a representative ice floe is investigated. Moreover, two alternative side shell waterline designs are considered for improving the ice-worthiness of the non-ice strengthened naval vessel: (1) a Lean Duplex (EN1.4062) design; and (2) the same Lean Duplex design with additional transverses.

2. Method

2.1. Ice load scenario

The considered ice load scenario has been defined in collaboration with the RNLN with the following assumptions:

- The vessel should be able to independently operate in ice-infested waters;
- Impact with a single ice floe is considered;
- An ice coverage of 60% is assumed;
- The maximum size of an encountered ice floe is 100 × 100 m;
- The floe consists of medium first-year ice with a thickness in the lower range according to the definition of JCOMM Expert Team on Sea Ice (2014).

The heavy shoulder glancing scenario used by the International Association of Classification Societies (IACS) polar class rules has been selected as scenario, see Figure 1. The ice loads are derived using the Direct Design for Polar Ships (DDePS)-2a model as described in SSC-473 (see, for example, Dolny (2017, 2018)).

2.2. Ice load model

The DDePS-2a model requires several ice properties as input. These are given in Table 1 and motivated below:

- **Ice floe length and width:** The ice floe length and width, $L \times B$, is taken as 100 × 100 m.
- **Ice thickness:** The ice thickness, h_{ice}, is 0.8 m which is in the lower range of the ice thickness expected for medium first-year ice as defined by JCOMM Expert Team on Sea Ice (2014).

CONTACT Sander Dragt sander.dragt@tno.nl

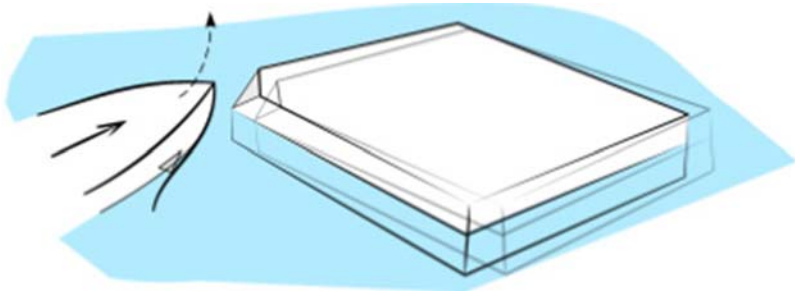

Figure 1. Finite ice floe shoulder glancing scenario. Copied from Dolny (2018). (This figure is available in colour online.)

Table 1. Overview of the selected ice floe parameters.

L × B [m × m]	h_{ice} [m]	ρ_{ice} [kg/m^3]	σ_f [MPa]	P_0 [MPa]	ex [-]	Φ [°]
100 × 100	0.8	920	0.8	2	−0.1	120

- **Ice density**: The density of the ice ρ_{ice}, is set to 920 kg/m^3, based on Timco and Weeks (2010) for first-year ice.
- **Ice flexural strength**: For the ice flexural strength, σ_f, a value of 0.8 MPa is taken. This is based on the range provided by Timco and Weeks (2010) and corresponds to a flexural strength that is in between the values of PC5 and PC6;
- **Nominal pressure and exponent**: For the present study an operational ice load is used instead of a design (e.g. 1 per 100 year) load. The nominal pressure P_0 is taken as 2 MPa and the exponent ex as −0.1, in consensus with Dolny (2017). The maximum allowed pressure has been capped to 30 MPa.
- **Ice wedge angle:** An ice wedge angle, φ, of 120° is assumed.

The DDePS-2a model requires geometrical parameters to define the interaction between ice floe and ship. The definition of the vessel and hull dimensions are provided in Figure 2. For the present work a typical 140 m long and 6000 ton naval vessel is considered. The value of the parameters are taken from the chosen impact location.

From the DDePS-2a model, the contact surface $A_{contact}$, normal force F_n, average pressure P_{avg} and the normal crushing depth ζ_n are obtained, see Figure 3. For structural analyses,

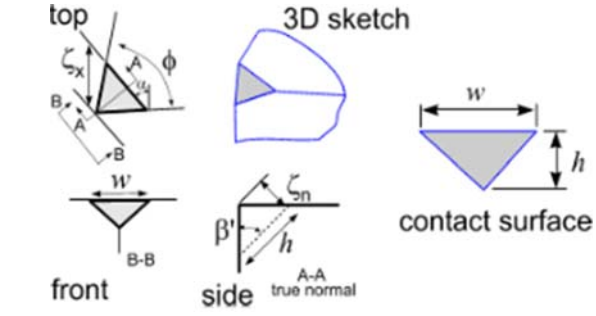

Figure 3. Top, front, side and isometric (3D) sketch with the relevant geometric definitions for the crushing process. Copied from Dolny (2018). (This figure is available in colour online.)

a rectangular contact surface is more readily applicable than a triangular contact surface. Therefore, the triangular load patch is converted to a rectangular load patch, see Figure 4.

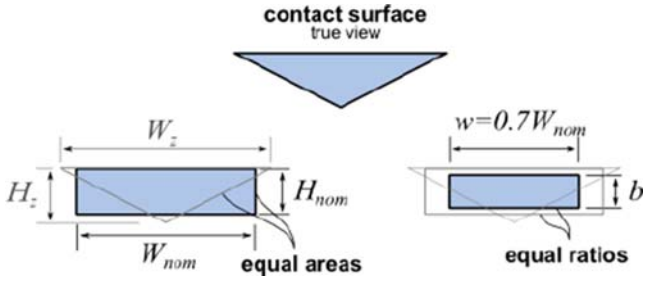

Figure 4. Conversion of the triangular contact surface to a rectangular load patch. Copied from Dolny (2018). (This figure is available in colour online.)

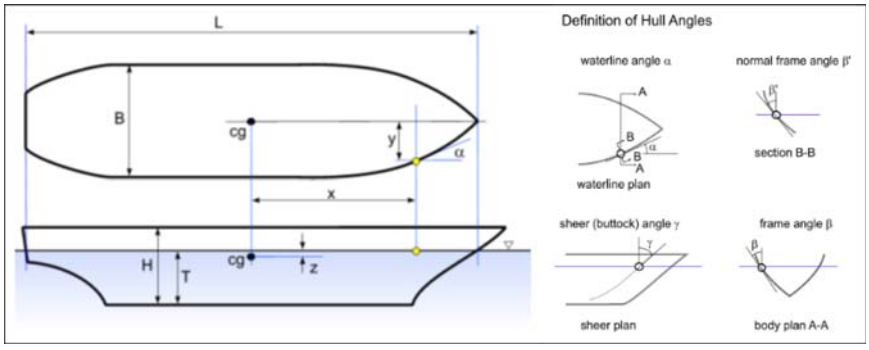

Figure 2. Vessel and hull dimensions. Adapted from Dolny (2018). (This figure is available in colour online.)

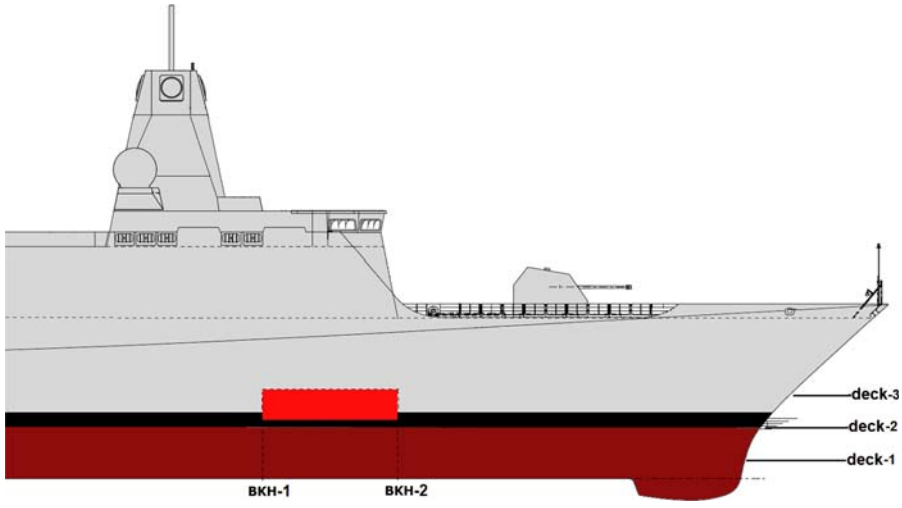

Figure 5. Illustration of the forward section of the considered naval vessel with the critical location indicated in red. The construction waterline (CWL) is about 0.8 m above the tweendeck. (This figure is available in colour online.)

Table 2. Overview of the two considered impact locations.

Case #	Name	Lengthwise location	Height wise location
1	L33	Just aft of BKH-2	At stiffener L33
2	L33+260	Just aft of BKH-2	260 mm above L33

The DDePS-2a implementation follows the model description by Dolny (2017, 2018) but for the flexural ice limit:

- Friction and dynamic effects are not considered.
- The quasi-static wedge angle independent model of the IACS Polar rules has been used.

2.3. Location of impact

To determine the initial point of impact, the critical location along the waterline of the vessel is determined. This location depends on both the local bending stiffness and the magnitude of the ice load. As both changes along the waterline, the location with the highest ratio between the ice load and the local bending stiffness is taken. This corresponds to the front shoulder at about ¾ of the length between perpendiculars (Lpp), see Figure 5.

The two impact locations that will be considered for the analysis are summarised in Table 2. Note that L33 is the first longitudinal stiffener above deck-2, spaced at 600 mm.

2.4. Acceptance criteria

To assess the severity of the deformations of the side shell structure, three acceptance criteria have been defined in collaboration with RNLN. The criteria are subdivided into two classes: visual and structural criteria:

- **The visual criteria** (e.g. dent) are deemed to be unacceptable, but there is no significant loss expected in the load carrying capacity of the shell structure.
- **The structural criterion** can be observed visually and have a consequence to the load carrying capacity of the side shell structure.

The first (visual) criterion is the out-of-plane plate deformation between stiffeners, see Figure 6. The criterion is defined by Equation (1). The criterion value c is set to 1.5% of the stiffener spacing.

$$y_P - \frac{y_{L1} + y_{L2}}{2} < c \tag{1}$$

The second (structural) criterion is the stiffener rotation. The criterion is defined by Equation (2), where is the criterion angle γ_c. The angle γ_c depends on the type of stiffener, see Figure 7.

$$\gamma < \gamma_c \tag{2}$$

The third (visual) criterion is the stiffener deformation between web frames, see Figure 8. The criterion is defined by Equation (3), where c is set to 1.0% of the web frame spacing. As a result, the criteria limits used for the various acceptance criteria depend

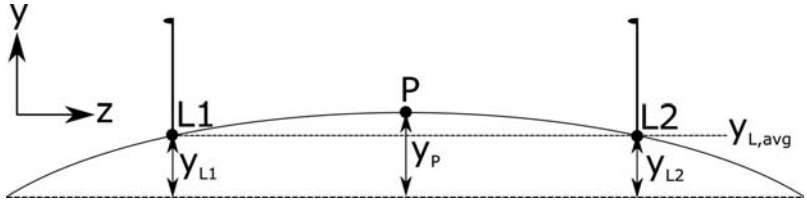

Figure 6. Displacements for assessing the out-of-plane plate deformation between stiffeners criterion. (This figure is available in colour online.)

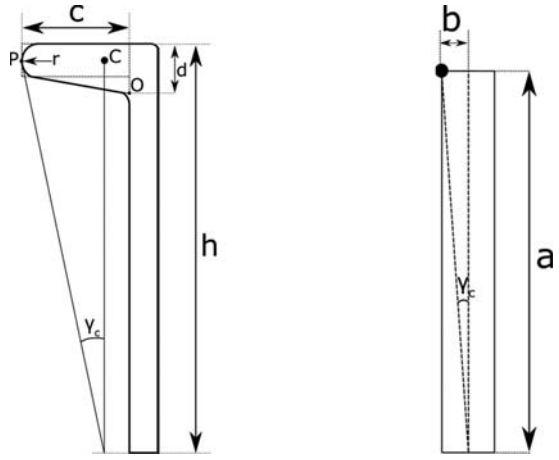

Figure 7. Definitions of the angle for the stiffener rotation criterion, γ_c, for a bulb flat (left) and a flat bar (right) stiffener. (This figure is available in colour online.)

on the scantlings of each design.

$$y_P - \frac{y_{W1} + y_{W2}}{2} < c \tag{3}$$

2.5. FE model: reference vessel design

For the reference vessel, the region of interest is the front shoulder at about ¾ Lpp. To allow for a sliding load and avoid boundary influence the model spans over 12 m, a multiple of the impact region. The deck-1 and deck-2 are modelled 2 and 3.5 m athwart, respectively. The height spans three decks. The defined modelling region is illustrated in Figure 9.

In the region of impact, bulb flat penetrations, bulb flat transitions and lug plates have been modelled.

The model is created in LS-Dyna and features a mesh (282,647 elements) consisting of a refined (element seed of 20 mm), coarse (element seed of 35 mm) and a transition region, see Figure 10. Since a sliding load is considered, the region of refinement spans 3.5 webframe spacings aft of BKH-2. The mesh consists mostly of quadrilateral shell elements. Triangular shell elements have been used where necessary. The shell elements use the default LS-Dyna element formulation 2 (Belytschko-Tsay), a shear factor of 5/6 and a Gauss integration scheme with 5 integration points over the thickness. The bulbs of the bulb flats have been modelled with beam elements.

The bulbs are modelled with beam elements with a user-defined integration rule, *INTEGRATION_BEAM. The beam has three integration points. The area definition and integration points are chosen such that the geometric properties (I_{yy}, I_{zz}, d_y and d_z) of the bulb flat are maintained.

The edges of the model are clamped (constraint in all translational and rotational Degrees of Freedom (DOF)) as shown in Figure 11.

The entire modelling region of the reference vessel consists of EH36 steel. The material properties and stress–strain curve used for this material are shown in Figure 12 and are as prescribed by the rules of Bureau Veritas (2019). The material is represented by the *MAT_PIECEWISE_LINEAR_PLASTICITY keyword.

2.6. FE model: Lean Duplex designs

Two alternative designs are investigated: a Lean Duplex and a Lean Duplex with transverses design. These designs aim at a

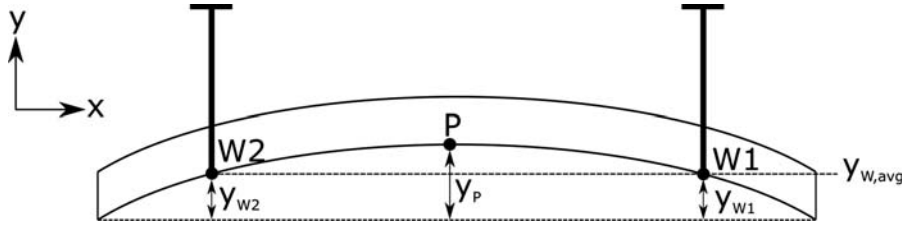

Figure 8. Displacements for assessing the stiffener deformation between web frames criterion. (This figure is available in colour online.)

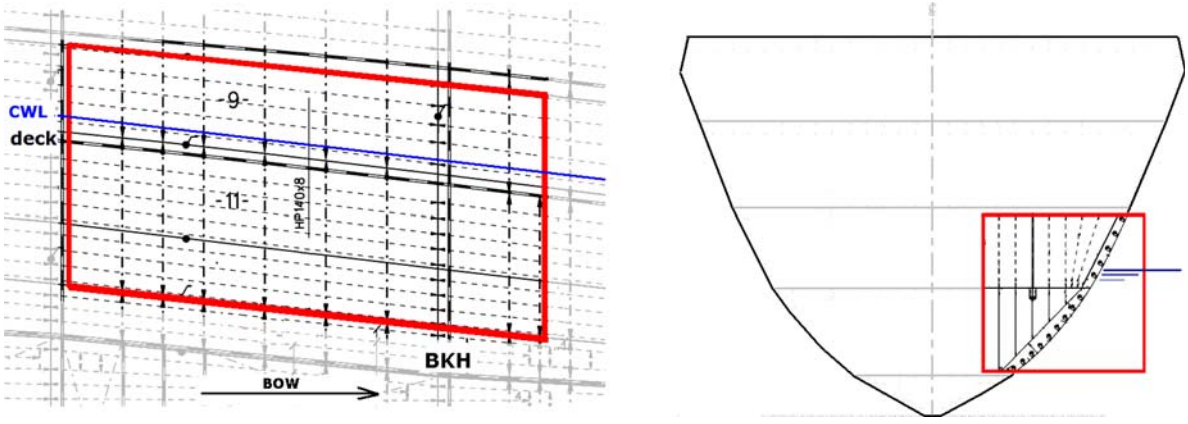

Figure 9. Longitudinal/shell expansion view (left) and transverse (right) view of the modelled region. (This figure is available in colour online.)

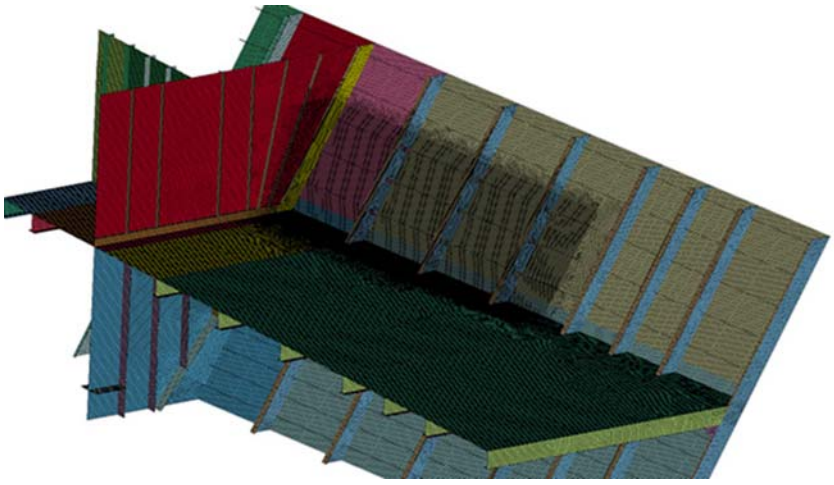

Figure 10. Mesh used for the numerical model of the reference design. (This figure is available in colour online.)

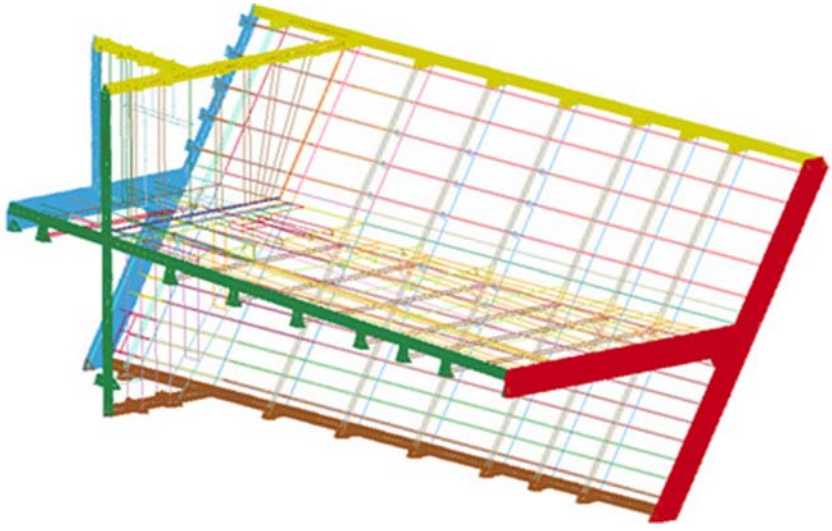

Figure 11. Edges (thick) where clamped boundary conditions are applied. (This figure is available in colour online.)

Parameter	Description	Value
E [GPa]	Young's modulus	210
v [-]	Poisson's ratio	0.3
ρ_{EH36} [kg/m^3]	Mass density	7850
ε_y^{eng} [-]	Engineering yield strain	1.69e-3
ε_f^{eng} [-]	Engineering failure strain	0.21
σ_y^{eng} [MPa]	Engineering yield strength	355
σ_{ult}^{eng} [MPa]	Engineering maximum strength	490

Plastic stress-strain curve

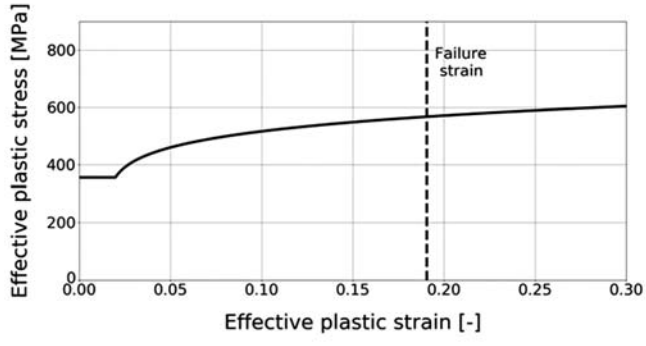

Figure 12. Material data for EH36 as used for the numerical models. Note that the plastic stress-strain curve is in terms of true plastic stress and strain. (This figure is available in colour online.)

highly elastic behaviour of the side shell to take ice loads in the ductile or 'shared energy' region, see Amdahl (2019) and DNV-GL (2019). The Lean Duplex designs extend from 1 m above the CWL to 2 m below CWL, and consists of 10 mm Lean Duplex (EN1.4062) plating and Lean Duplex 130 × 20 Flat Bars (FB) as longitudinal stiffeners, spaced at 450 mm. The flat bar penetrations through the web frames are closely fit, so the nodes of the FB130 × 20 and the web frames have been merged. Outside of the ice belt EH36 is used (just as for the reference model).

The Lean Duplex with transverses design adds FB50 × 20 stiffeners at every 300 mm between the web frames, running between the Lean Duplex stiffeners. All penetrations through the stiffeners are tight fit, so the nodes of the FB130 × 20 and the FB50 × 20 have been merged. The Lean Duplex and Lean Duplex with transverses designs are identical with the exception of the transverses. The alternative designs only alters the side shell and leaves the decks and bulkheads unchanged. The Lean Duplex designs are shown in Figures 13 and 14.

The mesh consists of a refined (element seed of 15 mm), coarse (element seed of 50 mm) and transition region, see Figure 15. The remaining bulb flats are out of the ice impact zone and only the webs are modelled. The models of the Lean Duplex designs use the same boundary conditions as for the model of the reference design.

The Lean Duplex material used in the ice belt is EN1.4062. The yield and ultimate engineering strengths and failure strain are obtained from ECISS/TC 107 (2016); and the Young's modulus and density are obtained from UGITECH (2010) for room temperature, see Figure 16.

2.7. Load

For all three models, the load is introduced by applying time and space dependent pressure on the relevant elements. The load magnitude and loaded elements correspond to the force exerted by, and the size of, the load patch from the DDePS-2a model for that particular time step. The load is applied as aft moving sliding load. Both the magnitude, size and location is updated every time step. The applied load (impetus) is independent of the model and only depends on the impact scenario (location and sailing speed).

For the reference vessel three sailing speeds are considered: 1, 2 and 3 m/s. For the Lean Duplex designs five sailing speeds are considered: 1, 2, 3, 4 and 5 m/s.

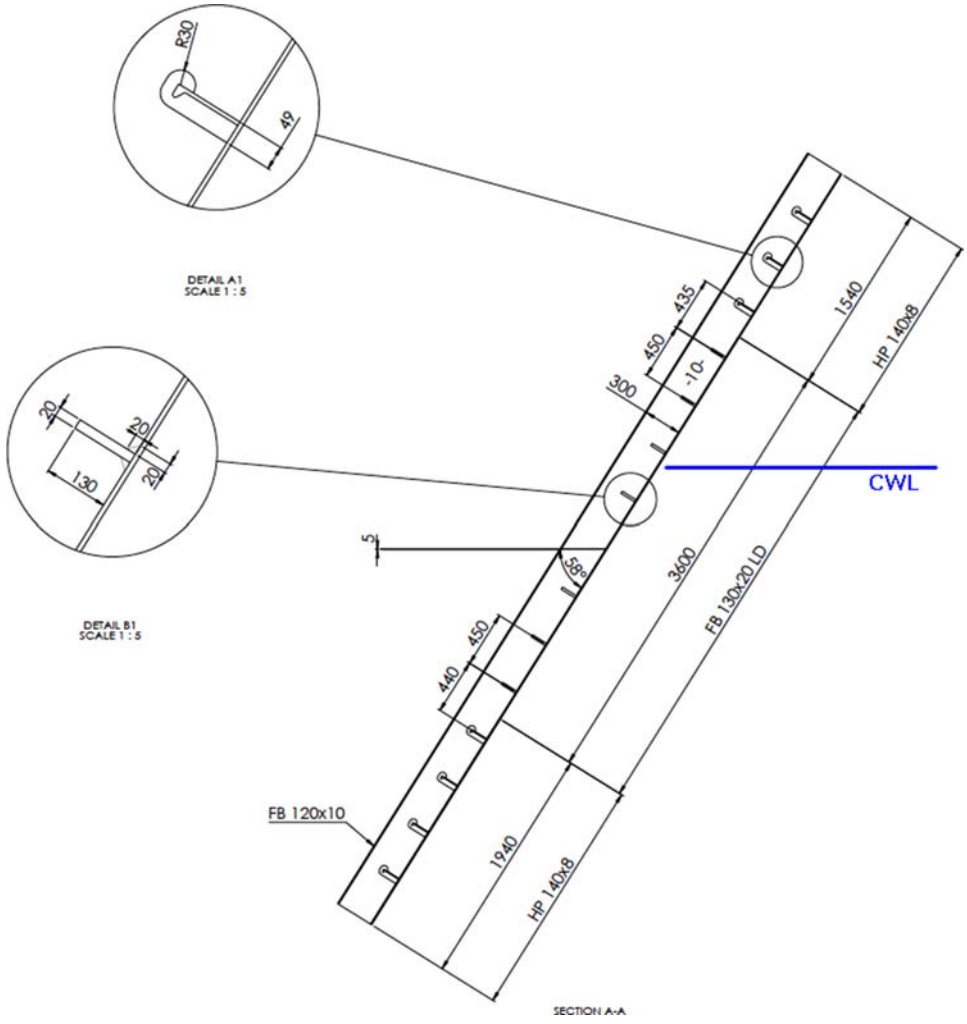

Figure 13. Side view of the side shell of the Lean Duplex designs. (This figure is available in colour online.)

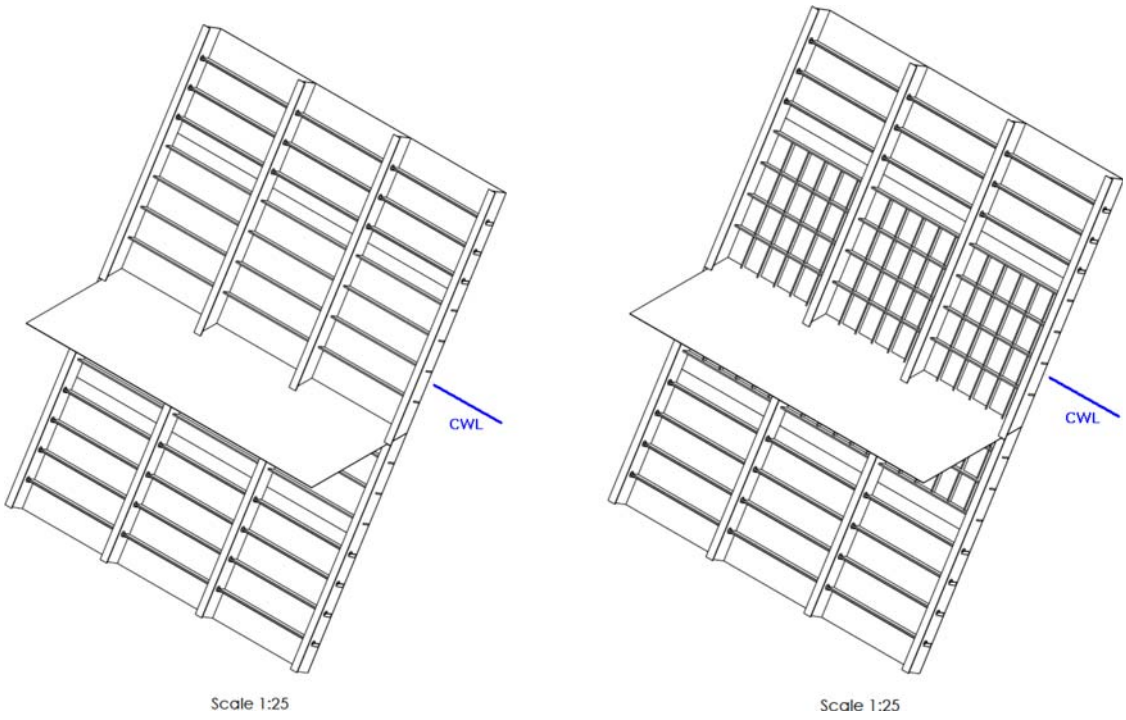

Figure 14. Isometric view of the Lean Duplex (left) and Lean Duplex with transverses (right) designs. (This figure is available in colour online.)

The load is introduced by using the *LOAD_SEGMENT_-SET keywords, for each loaded element. The pressure-time relations for each element at each time step t_i are determined with a load calculation procedure. For the procedure, the side shell is aligned with the x-axis, the y-axis with the side shell normal and the z-axis with the side shell in height-wise direction.

The patch dimensions are used to determine upon which elements pressure is applied at time t_i. On the elements a pressure is exerted such that the normal force is equal to the one obtained from the DDePS-2a.

Figure 17 illustrates the patch height, width, area and pressure as a function of time for a sailing speed of 2 m/s. The termination time of the analysis is longer than the application time of the load patch. This is to allow for an elastically unloaded end condition (residual deformations) to use in the criteria.

3. Results

The results of the simulations are summarised in Table 3 and visualised in Figure 18. The results show that the reference model exceeds one of the visual criteria at the lowest speed scenario of 1 m/s. Looking at the rotation of the stiffener, the reference model exceeds this criterion at the speed of 2 m/s. The residual deformations and plastic strains for this scenario

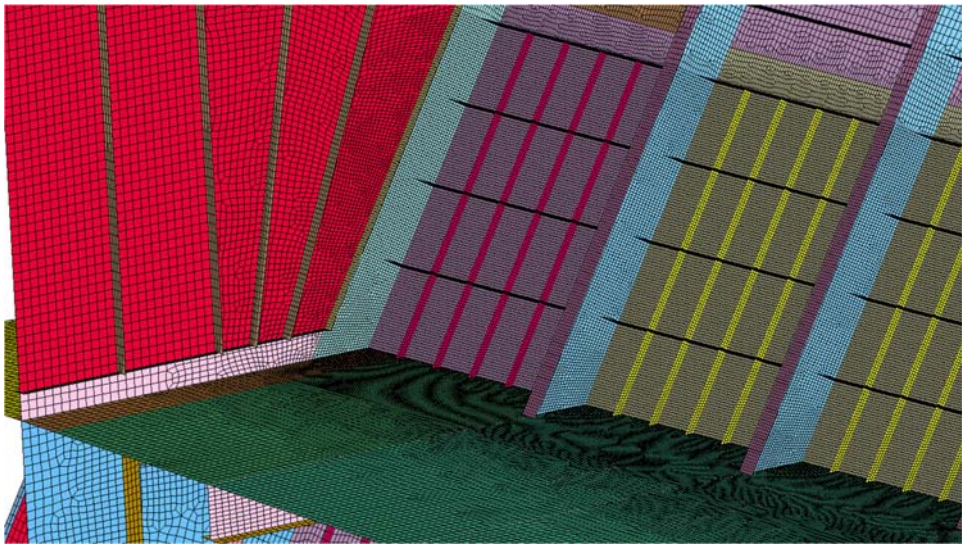

Figure 15. Mesh used for the numerical model of the Lean Duplex with transverses model. (This figure is available in colour online.)

Parameter	Description	Value
E [GPa]	Young's modulus	200
v [-]	Poisson's ratio	0.3
ρ_{LD} [kg/m^3]	Mass density	7800
ε_y^{eng} [-]	Engineering yield strain	2.25e-3
ε_f^{eng} [-]	Engineering failure strain	0.3
σ_y^{eng} [MPa]	Engineering yield strength	450
σ_{ult}^{eng} [MPa]	Engineering maximum strength	650

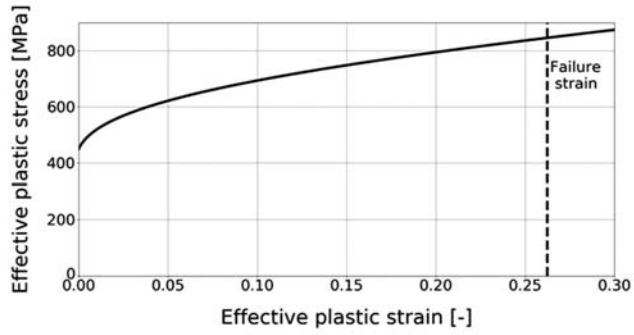

Figure 16. Material data for EN1.4062 (Lean Duplex) as used for the numerical models. Note that the plastic stress-strain curve is in terms of true plastic stress and strain. (This figure is available in colour online.)

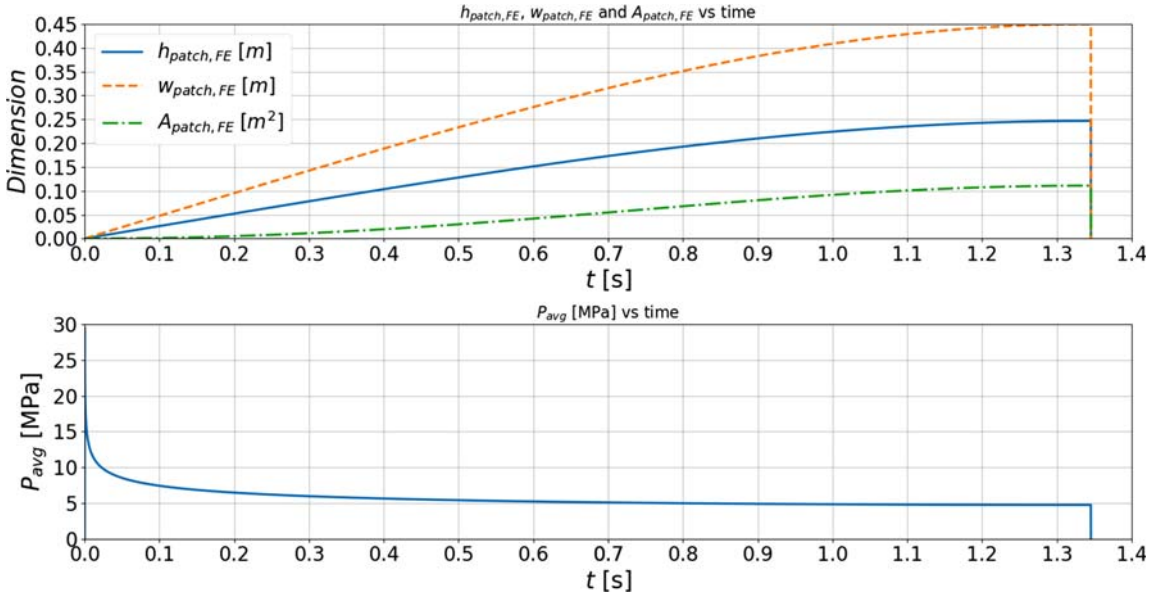

Figure 17. Patch height, width and area (top) and patch pressure (bottom) as a function of time. For the graphs a sailing speed of 2 m/s has been used. (This figure is available in colour online.)

are shown in Figure 19. In the figure, the bulkhead is hidden and the XZ-displacements are defined as $\sqrt{(\Delta x^2+\Delta z^2)}$. The residual deformations and plastic strains for impact at L33 +260 and a sailing speed of 2 m/s are shown in Figure 20.

The Lean Duplex design exceeds one of the visual criteria at a sailing speed of 2 m/s. The residual deformations and plastic strain for this case are shown in Figure 21. The stiffener rotation does not exceed the criterion at any speed.

The Lean Duplex with transverses design exceeds one of the visual criteria for the same scenario as for the Lean Duplex design (2 m/s, L33+260). The residual deformations and plastic strains are shown in Figure 22. The stiffener rotation does not exceed the criterion at any speed.

4. Discussion

Three aspects have been varied in the analyses: (1) sailing speed, (2) material and (3) structural layout of the side shell. This results in many findings regarding the loads, structural

Table 3. Summary of criteria results.

	Visual criteria/structural criterium exceeded?				
	1 m/s	2 m/s	3 m/s	4 m/s	5 m/s
Reference	Visual	Visual & structural	Visual and structural	N/A	N/A
Lean Duplex	None	Visual	Visual	Visual	Visual
Lean Duplex with transverses	None	Visual	Visual	Visual	Visual

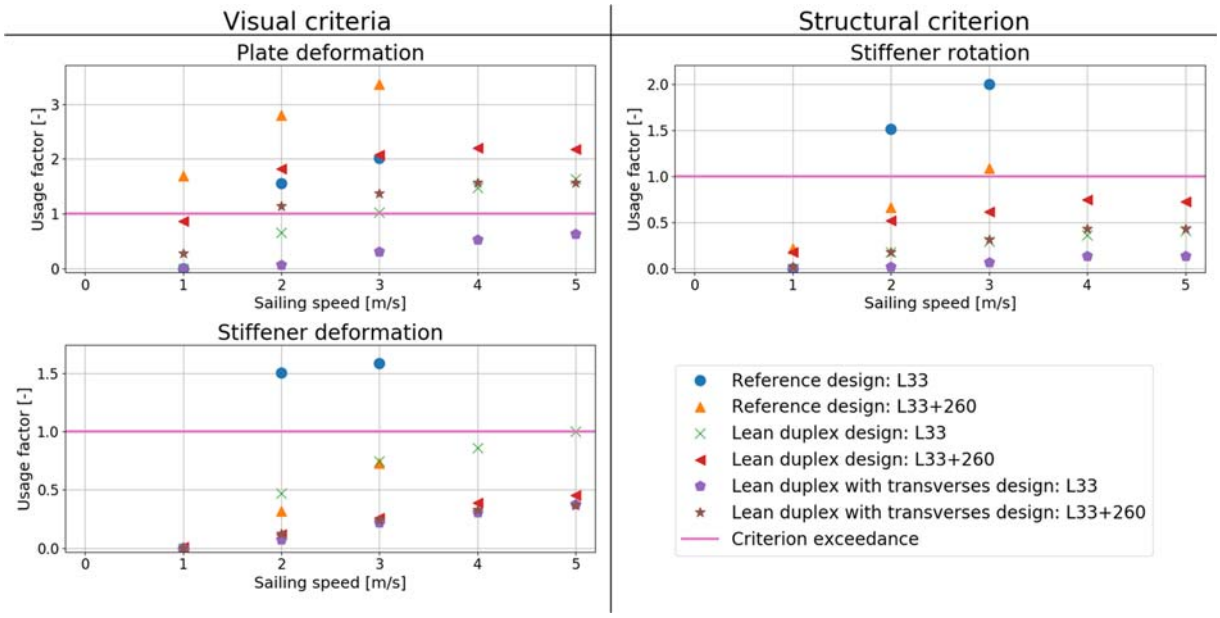

Figure 18. Usage factors for the reference, Lean Duplex and Lean Duplex with transverses models per criterion. The usage factor is the ratio between the value of the criterion and the criterion limit. A value greater than 1 corresponds to exceedance of the criterion. (This figure is available in colour online.)

behaviour and absorbed energy. The most interesting aspects will be discussed.

4.1. Sailing speed

Figure 23 shows the effect of the sailing speed on the magnitude and spatial distribution of the force over the impact duration, as described by the DDePS-2a ice model. With higher speeds, the maximum force increases up to the flexural limit after which it remains constant. This explains the plateau seen in the usage factors at high speeds (see Figure 18). Furthermore, the location of the hull that experiences the highest (sliding) load is depending on the sailing speed. This means that a different starting position could lead to different deformations. Therefore, it is recommended to investigate a range of impact locations.

4.2. Lean Duplex material

For two of the considered models EN1.4062 Lean Duplex has been used in the region of impact and for one of the models EH36. Compared to EH36, Lean Duplex has a higher yield strength, does not exhibit a yield plateau and exhibits more hardening. These effects contribute to the reduced plastic deformation for the same absorbed energy for the Lean Duplex models with respect to the reference design.

The results presented in this work feature both a different material and updated structural arrangement. To show the influence of the material, the constitutive material behaviour of Lean Duplex and EH36 are plotted in Figure 24. To illustrate the improved energy absorption capability, the strain required to dissipate an equal amount of energy is shown for EH36 and Lean Duplex. However, note that this behaviour is expected purely from a material point of view. The structural arrangement and behaviour, the different material aspects and the interaction between these aspects cannot be separated from the results of the analyses.

4.3. Structural layout

The Lean Duplex models have several structural updates compared to the reference model that improve the ice worthiness of the vessel. First of all, thick symmetric profiles are used for high rotational stability, improving the tripping behaviour. Second, the reduced stiffener height leads to a reduction in bending stress. Thirdly, the stiffener spacing is reduced from 600 to 450 mm, reducing the effective plate width in between stiffeners. Finally, stiffener penetrations (due to tight fit) are removed, this removes stress concentrations but does not increase the load carrying capacity of the stiffened plate.

The added transverses in the Lean Duplex with transverses model further increases the bending stiffness of the side shell and adds more material to be loaded elastically. This reduces the deformation of the side shell and stiffeners, but not to the extent that the technical safe limit speed increases.

4.4. Combined effect of modified material properties and structural layout

The internal energies for the L33+260 at 2 m/s scenario are shown in Figure 25 for the three models. The applied load (impetus) is the same for all three models. It can clearly be seen that the energy absorption is the highest for the reference design, second for the Lean Duplex design and then for the Lean Duplex with transverses design. This is explained by the Lean Duplex designs showing less

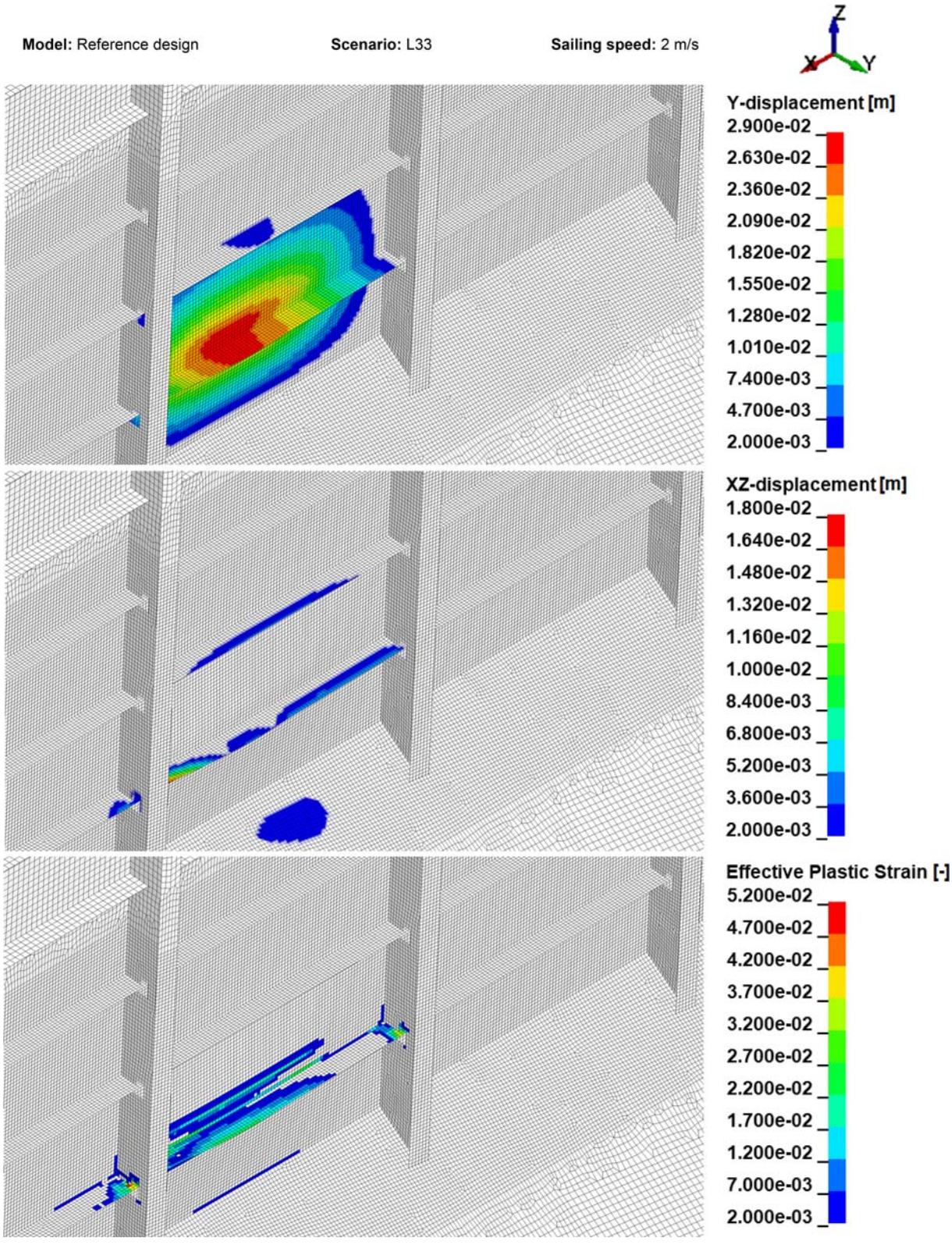

Figure 19. Results reference design for impact at L33 and sailing speed of 2 m/s. (This figure is available in colour online.)

deformation, hence less plastic work energy. Both the changed material properties and the modified structural arrangement contribute to the improved structural performance, however, the contribution cannot be separated. The addition of transverses decreases the plasticity and deformation further.

As stated before, it is not possible to separate the effect of the material and the structural layout. For future work it is of interest to perform additional simulations where all three structural layouts are simulated for the EH36 and Lean Duplex material. This will provide insight into the influence of change material only and the influence of the structural layout only.

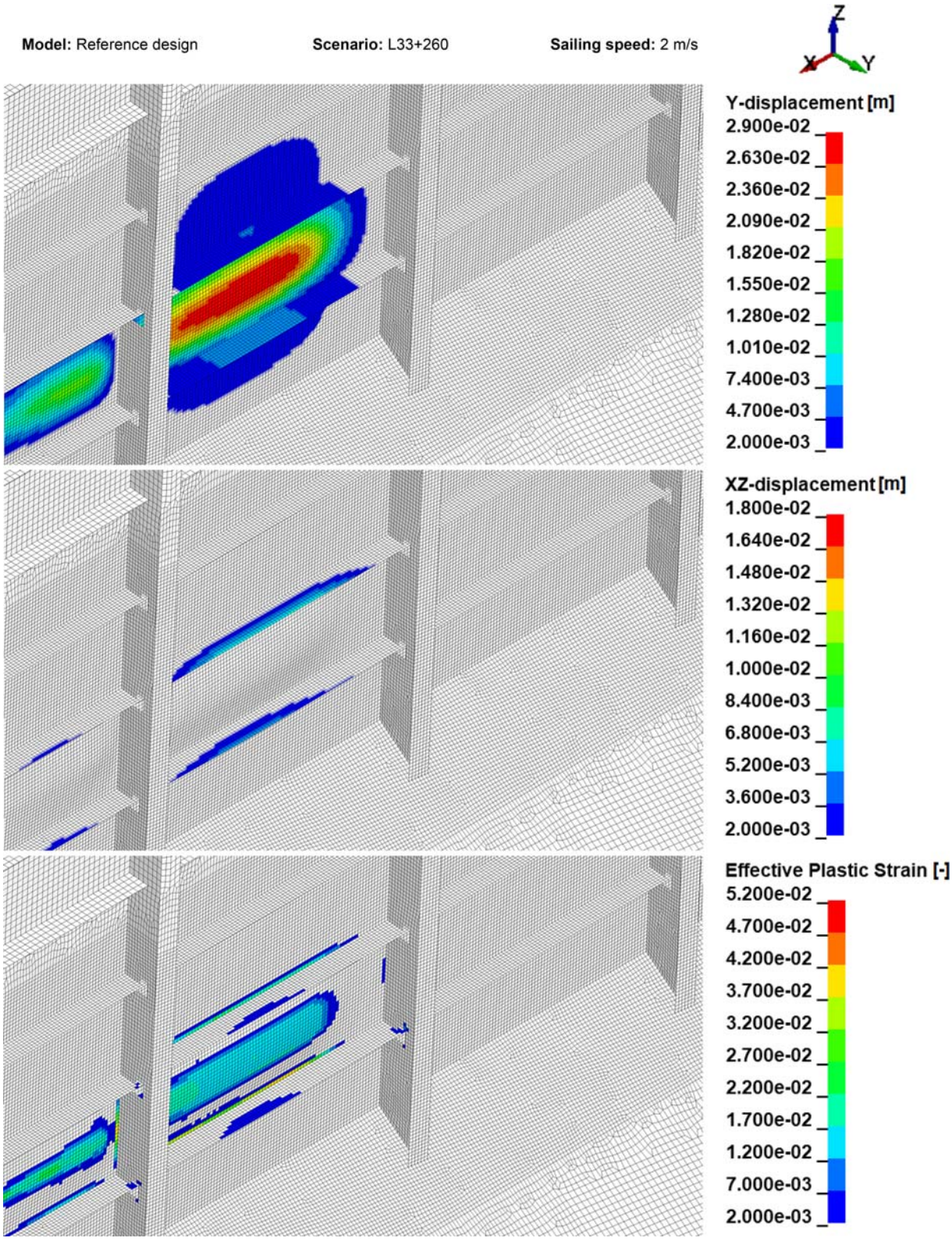

Figure 20. Results reference design for impact at L33+260 and sailing speed of 2 m/s. (This figure is available in colour online.)

5. Conclusions

For the considered designs and the selected ice impact scenario, ice impact for the reference design will lead to visual deformations, even at low sailing speeds (1 m/s). At slightly higher sailing speeds (2 m/s and up), stiffener rotation exceeds the structural criterion and a reduction of side shell load carrying capacity is expected. Changing the structural layout and the material (EN1.4062, Lean Duplex) reduces the deformation of the side shell structure. The first exceedance of the visual criterion is at 2 m/s, the structural criterion is not exceeded at all. This is an improvement with respect to the reference design. Permanent deformations, however, are still

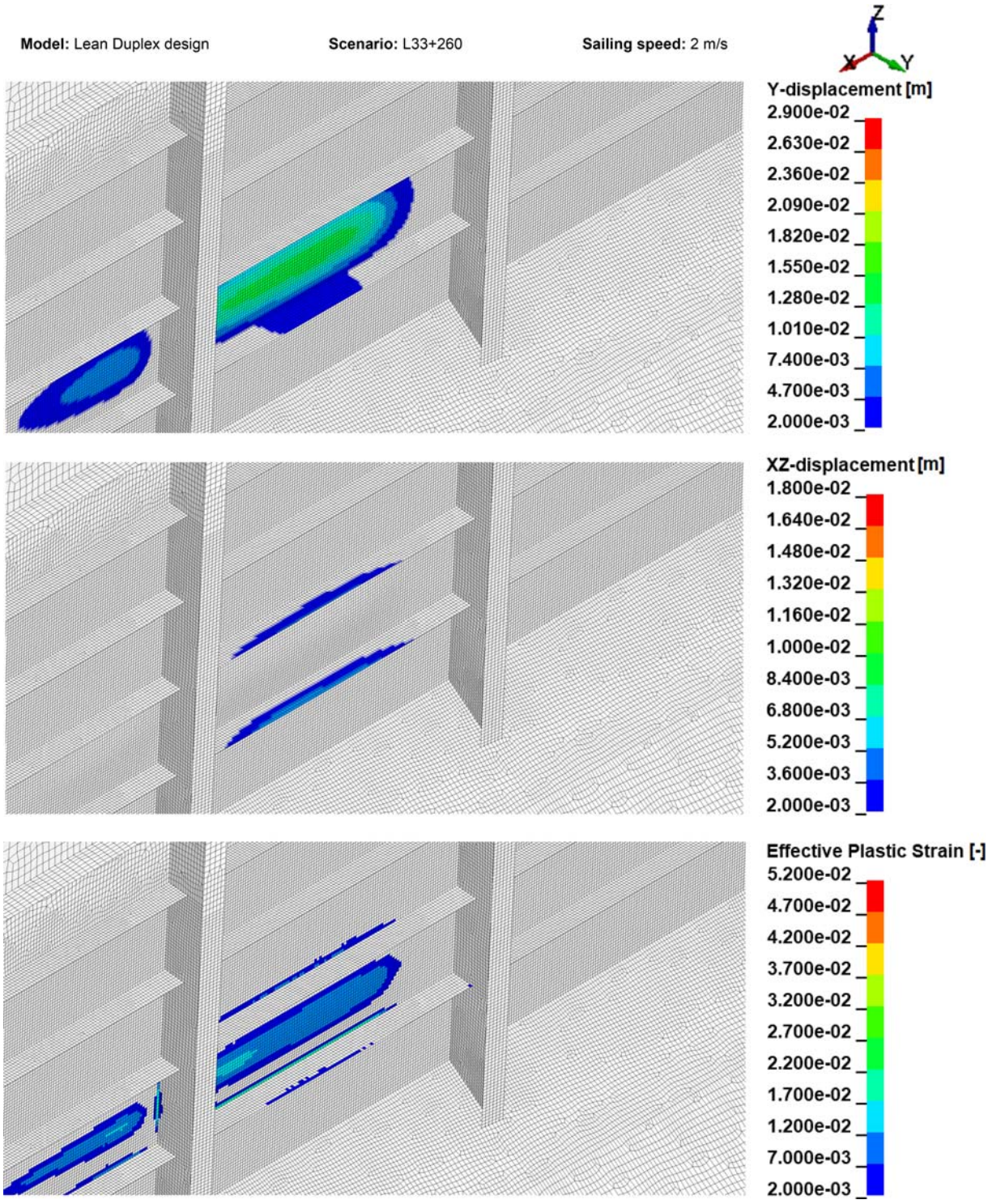

Figure 21. Results Lean Duplex design for impact at L33+260 and sailing speed of 2 m/s. (This figure is available in colour online.)

to be expected when these non-ice strengthened ships are operating in ice-infested waters. It is shown that both the material modification and the structural design improvement attribute to the increased ice impact resistance.

6. Recommendations

For determining the ice load, a deterministic scenario has been selected based on assumptions and reasonable values for ice parameters from literature. It is argued that this is valid to investigate the effect of different structural layouts. Table 4 provides a sensitivity overview of the various ice parameters used by the DDePS-2a model for a sailing speed of 2 m/s. The reference ('as used') is the case used in this report for determining the ice loads. From the table it can be seen that a change in the ice parameter can have a significant impact on the ice load. For design purposes, or to provide advice on operations in ice invested waters, a wide range of realistic ice

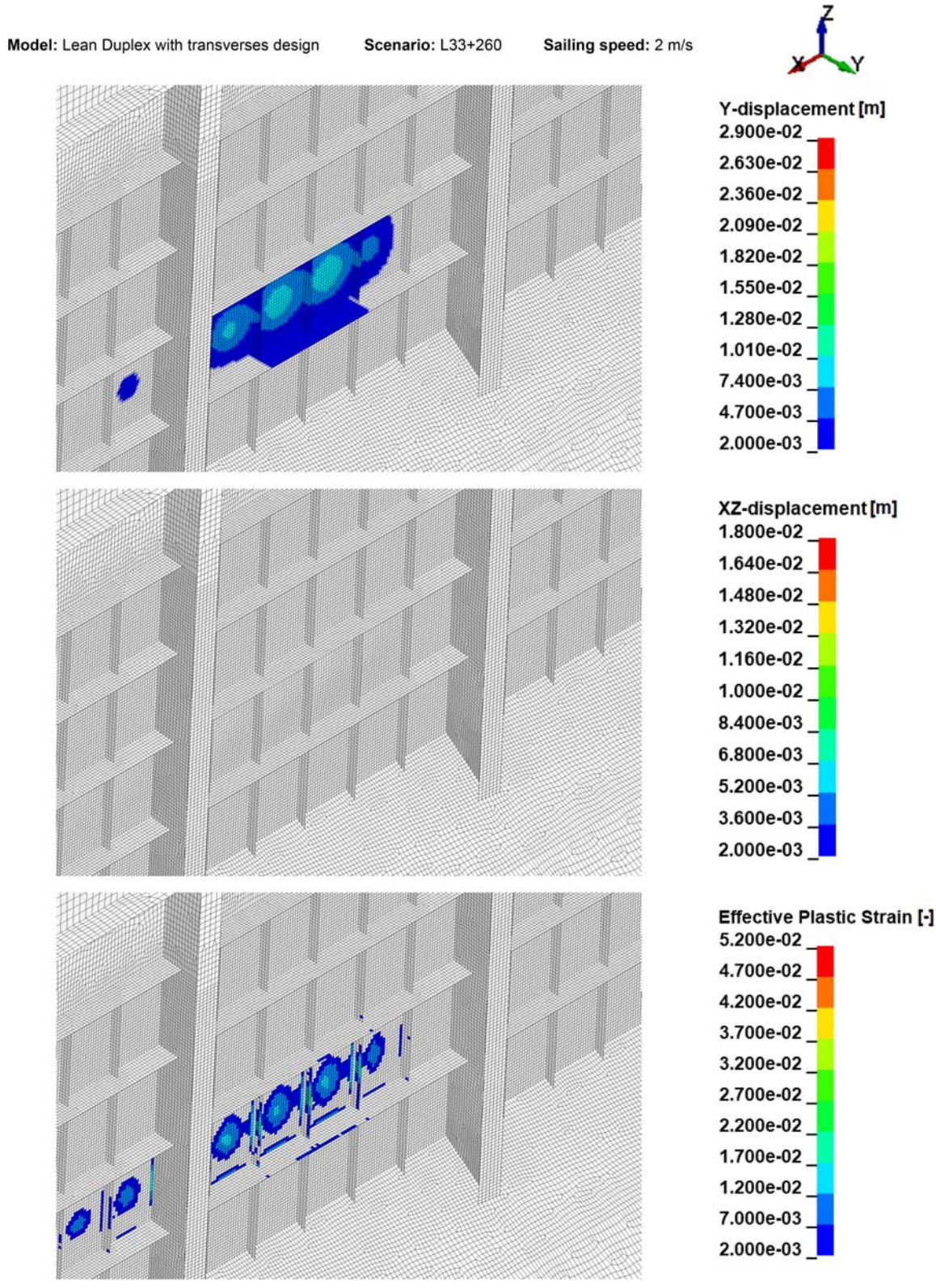

Figure 22. Results Lean Duplex with transverses design for impact at L33+260 and sailing speed of 2 m/s. (This figure is available in colour online.)

scenarios have to be investigated. Probabilistic methods or design loads derived for such approaches are recommended.

The ice load is determined with the DDePS-2a model that assumes a rigid side shell. This means that the only energy dissipation is due to ice crushing. However, for an elastic side shell energy is also dissipated by the deformation of the side shell. Therefore, assuming a rigid side shell will overestimate the magnitude of the normal force (and of the applied pressure). It is recommended to look into methods to incorporate the effect of the elastic hull on the ice load.

The DDePS-2a model used for determining the ice load is a low-fidelity model with several simplifications such as a wedge

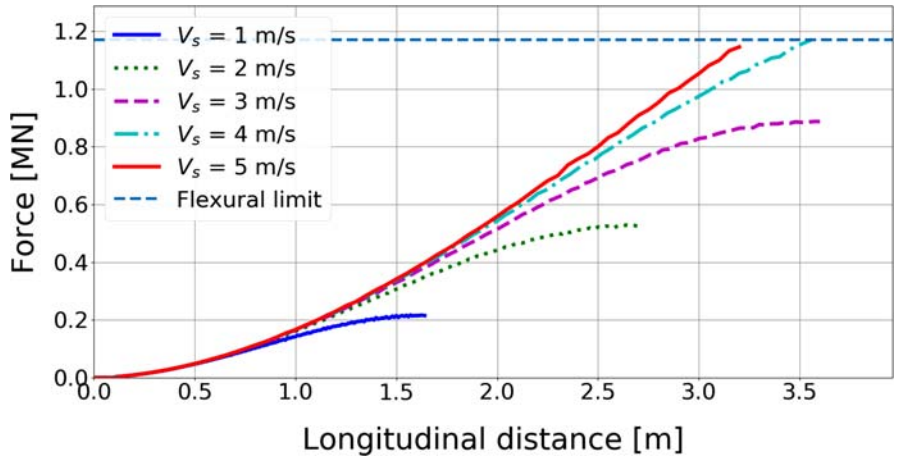

Figure 23. The normal force as a function of the longitudinal distance for the considered sailing speeds. The normal force is obtained from the FEM analysis. (This figure is available in colour online.)

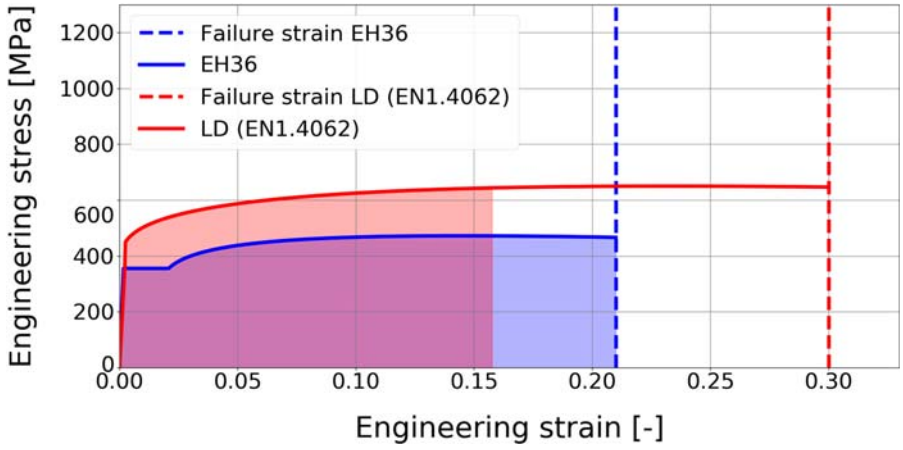

Figure 24. Strain to absorb equal energy for EH36 and Lean Duplex. (This figure is available in colour online.)

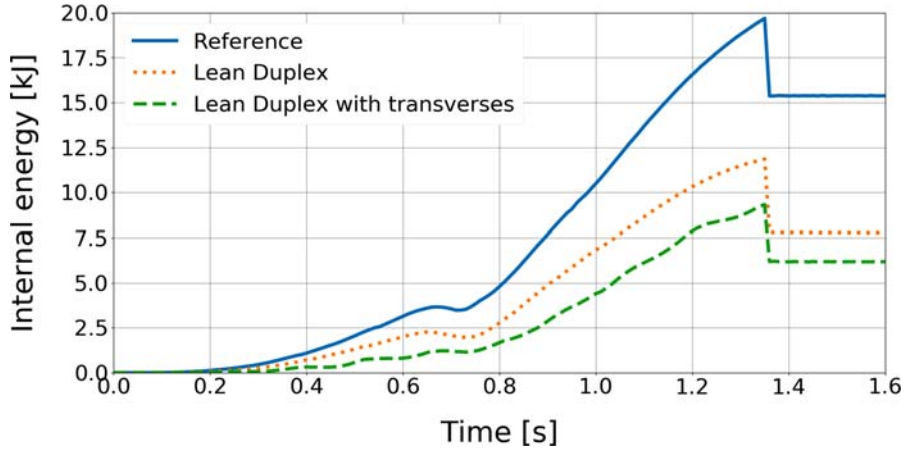

Figure 25. Internal energy for the reference, Lean Duplex and Lean Duplex with transverses models for impact at L33+260 and sailing speed of 2 m/s. (This figure is available in colour online.)

Table 4. The sensitivity of the normal crushing depth ζ_n, the normal force F_n, contact area $A_{contact}$ and the average pressure P_{avg} on the ice parameters required for the DDePS-2a model. A sailing speed of 2 m/s is used.

Parameter	Parameter range		ζ_n [m]	F_n [MN]	$A_{contact}$ [m^2]	P_{avg} [MPa]
h_{ice} [m]	0.4–1.4	**Low**	0.12	0.19	0.07	2.49
		High	0.16	0.28	0.11	2.61
		As used	0.14	0.24	0.10	2.53
$L \times B$ [m x m]	50 × 50–150 × 150	**Low**	0.10	0.13	0.05	2.47
		High	0.16	0.30	0.12	2.71
		As used	0.14	0.24	0.10	2.53
ρ_{ice} [kg/m^3]	880–940	**Low**	0.14	0.23	0.09	2.53
		High	0.15	0.24	0.10	2.54
		As used	0.14	0.24	0.10	2.53
σ_f [MPa]	0.4–1.2	**Low**	0.14	0.24	0.04	2.53
		High	0.14	0.24	0.16	2.53
		As used	0.14	0.24	0.10	2.53
P_0 [MPa]	1.0–6.0	**Low**	0.10	0.19	0.04	1.20
		High	0.19	0.36	0.16	8.21
		As used	0.14	0.24	0.10	2.53
ex [-]	−0.1 – −0.7	**Low**	0.04	0.24	0.01	2.53
		High	0.14	0.47	0.10	58.1
		As used	0.14	0.24	0.10	2.53
φ [deg]	60–150	**Low**	0.11	0.17	0.06	2.46
		High	0.21	0.31	0.13	2.63
		As used	0.14	0.24	0.10	2.53

angle independent ice flexural limit, and neglecting dynamic effects, friction and horizontal relieving or negating stresses. It is recommended to consider these effects in future work.

Two impact locations have been considered. These two locations are chosen as they represent two extreme cases: on and in between longitudinal stiffeners. Other locations, for example at or just above the deck or a bulkhead, have not been considered. Furthermore, no changes are made to the start location of the impact and thus the structural features that are encountered at different stages of the event. For establishing a risk profile ice impacts on non-ice-strengthened vessels, a larger range of impact starting locations has to be considered.

For future work it is recommended to perform additional simulations where all three structural layouts are simulated for the EH36 and Lean Duplex material. This will provide insight into the influence of change material only and the influence of the structural layout only.

Lastly, it is recommended to look into experiments that validate the magnitude of the ice load when applied to an elastic hull and to validate the response of the elastic hull to the ice load.

Acknowledgements

This work is enabled by the RNLN and the authors thank the partners of the NATO workgroup AVT-300, Naval Ship Maneuvrability in Ice, for their support. Moreover, the authors would like to thank Professor Claude Daley (Memorial University of Newfoundland) for providing the DDePS-2a model in the form of an excel sheet.

Disclosure statement

No potential conflict of interest was reported by the author(s).

ORCID

Mark Bobeldijk http://orcid.org/0000-0002-6768-4035

References

Amdahl J. 2019. Impact from ice floes and icebergs on ships and offshore structures in Polar regions. IOP Conf Ser: Mater Sci Eng. 700 (012039):1–16.

Bureau Veritas. 2019. NR 216: rules on materials and welding for the classification of marine units. Paris La Defense Cedex: Bureau Veritas.

Daley CG. 2015. Ice impact capability of DRDC notional destroyer. St. John's: Memorial University of Newfoundland.

DNV-GL. 2019. DNV-RP-C204: design against accidental loads. Høvik: DNV-GL.

Dolny JR. 2017. A technical methodology for establishing structural limitations of ships in pack ice. St. John's: Memorial University of Newfoundland.

Dolny JR. 2018. SSC-473: Methodology for defining technical safe speeds for light ice-strengthened government vessels operating in ice. Washington: Ship Structure Committee (SSC).

ECISS/TC 107. 2016. EN 10028-7: flat product made of steels for pressure purposes – Part 7: stainless steels. Brussels: CEN.

JCOMM Expert Team on Sea Ice. 2014. WMO-No.259: WMO sea-ice nomenclature, volumes I, II and III. Geneva: WMO.

Quinton BWT, Daley CG.. 2010. Effect of moving ice loads on the plastic capacity of a ship's structure.International Conference and Exhibition on Ships and Structures in Ice (Icetech).Anchorage.

Quinton BWT, Daley CG, Gagnon RE.. 2012. Realistic Moving Ice Loads and Ship Structural Response.International Ocean and Polar Engineering Conference (ISOPE).Rhodes.

Timco GW, Weeks WF. 2010. A review of the engineering properties of sea ice. Cold Reg Sci Technol. 60(2):107–129.

UGITECH. 2010. Technical datasheet: UGI 4062. Ugine Cedex: UGITECH.